

On Dynamics of an Externally Pressurized Air Bearing with High Values of Clearance: Effect of Mass Flow Rate

Abdurrahim DAL, Tuncay KARAÇAY

Abstract—Externally pressurized gas lubricated bearings with small clearance have some practical disadvantages such as difficulties in manufacturing process, price, assembly etc. and so, they don't become widespread. These disadvantages can be solved with use of higher values of clearance in the bearing. But bearings with high clearance have low load carrying capacity in the contrary. The load carrying capacity can be increased by using high value of orifice diameter or more orifice, in other words with higher mass flow rate. In the literature general accepted value for clearance is lower than 50 μm and there is a limited number of study the dynamics of externally pressurized air bearing especially with high values of clearance. In this study the flow between shaft and rotor was modelled using Reynold's Equation which is fluid equation of motion and this model is solved by Alternating Direction Implicit (ADI) numerical solution method, in order to investigate the dynamic of an externally pressurized gas lubricated bearing with increased clearance.

Index Terms—Externally pressurized air bearing, rotor dynamics, Reynold's equation, mass flow rate

I. INTRODUCTION

IN externally pressurized air bearings rotor is supported by air. The air prevents direct surface contacts and reduces the friction between the surfaces of the bearing and the rotor. So, they are suitable for high speed application. Generally externally pressurized air bearing is manufactured with small value of clearance. But the bearings with small clearance have some practical disadvantages such as difficulties in manufacturing process, price and assembly. So, externally pressurized air bearing cannot become widespread. On the other hand, the externally pressurized air bearings with higher value of clearance have low load carrying capacity. But the load carrying capacity can be increased with higher mass flow rate.

Manuscript received March 14, 2014. This work was supported in part by the The Scientific and Technology Research Council of Turkey under Grant No 112M847.

A. DAL is with the Gazi University Mechanical Engineering Department, Ankara, 06570 Turkey (phone: +90 312-582-3464, e-mail: abdurrahimdal@gazi.edu.tr).

T. KARAÇAY is with Gazi University Mechanical Engineering Department, Ankara, 06570 Turkey (e-mail: karacay@gazi.edu.tr).

Mass flow rate is strongly associated with operational parameter such as supply pressure, orifice diameter and number of orifice. So, over the past decades, many investigations have been investigated on the operational condition on dynamics of the externally pressurized gas lubricated bearing. Fleming et al., performed a small eccentricity analysis on a bearing having two feeding planes and they obtained load and attitude angle with speed at different supply pressure and feeding parameter for steady state [1]. Fourka and Bonis analyzed the influence of feeding system type on the performance of externally pressurized gas bearings. They compared the optimum characteristics regarding load capacity, stiffness and flow rate of an air thrust bearing which can be obtained by using different kinds of multiple inlets specifically designed with orifices or porous compensation. They concluded that optimum performance may be achieved for each of these different feeding systems, which depend on an optimum number of inlets, position of orifices, or permeability coefficient of the porous material [2]. Renn and Hsrao in an experimental and CFD study, investigated on the mass flow-rate characteristic through an orifice-type restrictor in aerostatic bearings which radial clearances are 12 and 18 μm . They concluded that the mass flow-rate characteristic through an orifice is different from that through a nozzle and the conventional model to determine the mass flow-rate through an orifice-type restrictor in aerostatic bearings may have to be updated to the proposed new model for more precise design and modelling of the gas-lubricated aerostatic bearings. [3]. Lo et al. discretized Reynold's equation by use Newton method and investigated load carrying capacity and stiffness for different supply pressure, L/D ratio and clearance [4]. Colombo et al. considered, in a theoretical study, the effect of orifice feeding and supply pressure on the load capacity and stiffness externally pressurized gas bearings which have one and two sets of orifices and 38 μm radial clearance [5]. They concluded that the load capacity and stiffness could be improved with high supply pressure and increased orifice diameter. Colombo et al. compared radial stiffness and pressure distribution for three externally pressurized gas bearing at different air consumption rates [6]. Chen et al. investigated stiffness of various geometric designs of aerostatic journal bearings for high-speed spindles under different operating conditions. They evaluated stiffness experimentally using the relationship of force and displacement at different supply pressures. They concluded that the stiffness could be improved with high supply pressure, high L/D ratio and increased orifice diameter [7].

Belforte et al. considered, in a experimental study the effect of discharge coefficient on the pressure distribution with different supply pressure with two types of air feeding systems which were annular orifices and simple orifices with feed pocket. They investigated air consumption and pressure distribution as a function of supply pressure and air gap height. They obtained experimental formula for discharge coefficient [8].

Many studies on effect of mass flow rate on the dynamics of an externally pressurized gas lubricated bearing are presented in literature [2]-[8]. But literatures about effect of mass flow rate are generally analyzed for small clearance. Externally pressurized gas lubricated bearings have low load carrying capacity for high clearance. However the load carrying capacity can be increased by increasing the diameter of orifice or the number of orifice. In other words the load carrying capacity may be increased with higher mass flow rate. In this study the effect of mass flow rate is investigated on the dynamic of an externally pressurized gas lubricated bearing with increased clearance. Pressure distribution which is important parameters of externally pressurized gas lubricated bearing was modelled Reynold's Equation which is known fluid equation of motion and solved using by Alternating Direction Implicit (ADI) numerical method. Dynamics of rotor is investigated for different supply pressure, different orifice diameter and also number of orifice.

II. MATHEMATICAL MODEL

The externally pressurized air bearing-rotor system, geometrical parameters of bearing (length, diameter etc.) and coordinate system used in modelling are illustrated in Fig. 1. Radial motion of the rotor could be modelled in two degree of freedom using cartesian coordinates and given in (1). In this model it is assumed that rotor does only have axial motion. Right hand side of the equations are zero because the rotor was assumed balanced and there is no external force applied it.

$$\begin{aligned} m\ddot{x} + F_x &= 0 \\ m\ddot{y} + F_y &= 0 \end{aligned} \quad (1)$$

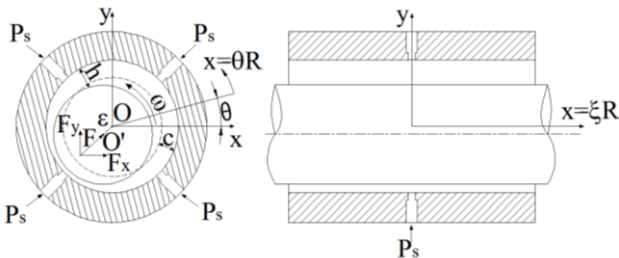


Fig. 1 Configuration of the externally pressurized air bearing

Reynold's equation could be given as in (2) using dimensionless parameters (see Fig. 1);

$$\begin{aligned} p &= P / P_a, \quad h = cH, \quad x = R\theta, \quad z = R\xi, \\ U &= r\omega, \quad \Lambda = \frac{6\mu\omega}{P_a} \left(\frac{R}{c}\right)^2, \quad \sigma = \frac{12\mu}{P_a} \left(\frac{R}{c}\right)^2 \end{aligned}$$

$$\frac{\partial}{\partial \theta} \left[H^3 P \frac{\partial P}{\partial \theta} \right] + \frac{\partial}{\partial \xi} \left[H^3 P \frac{\partial P}{\partial \xi} \right] + Q = \Lambda \frac{\partial}{\partial \theta} (PH) + \sigma \frac{\partial}{\partial t} (PH) \quad (2)$$

where P_a is the atmospheric pressure, H is the dimensionless film thickness function (6), c is the radial clearance, R is the radius of bearing and Q which is given in (3) is mass flow rate.

$$Q = \Gamma_0 P_s H \Phi(P) \quad (3)$$

In the mass flow rate (3) dimensionless feeding parameter, orifice function and dimensionless bearing gap are defined in (4), (5) and (6) respectively;

$$\Gamma_0 = \frac{12\pi d_0^2 \mu \sqrt{R^0 T^0}}{P_a c^2 \Delta \theta \Delta \xi} \quad (4)$$

$$\Phi(P) = \begin{cases} \sqrt{\frac{2k}{k-1} \left[\left(\frac{p_d}{p_u}\right)^{\frac{2}{k}} - \left(\frac{p_d}{p_u}\right)^{\frac{k+1}{k}} \right]} & \text{for } 1 > \frac{p_d}{p_u} \geq r_p \\ \frac{2k}{k+1} \left(\frac{2}{k+1}\right)^{\frac{1}{k-1}} & \text{for } \frac{p_d}{p_u} < r_p \end{cases} \quad (5)$$

$$H(\theta) = 1 - \epsilon \cos(\theta), \quad \epsilon = \frac{1}{c} \sqrt{e_x^2 + e_y^2} \quad (6)$$

where r_p is the critical pressure ratio, p_d is pressure of orifice exhaust, p_u is pressure of orifice inlet, k is the specific heat ratio and d_0 is the orifice hole diameter.

III. NUMERICAL ANALYSIS

A. Pressure Distribution

Reynold's equation which gives the pressure distribution between the rotor and the bearing is in the form of parabolic differential equation and this equation could be solved numerically. In this study the Reynold's equation is solved by alternating direction implicit (ADI) using the scheme which is given Appendix-A. However ADI method inherently has stability and convergence problems [9]-[13]. Especially if the radial clearance is increased, these problems become more severe. In this study a convergence criteria is defined in the routine of ADI as given in (10) in order to guaranteed the develop of fluid (air) flow within the gap.

$$\frac{|P_{i,j}^{n+1} - P_{i,j}^n|}{P_{i,j}^{n+1}} \leq 10^{-6} \quad (7)$$

If pressure function is $P(\xi, \theta)$, the boundary condition could be summarized as follows;

- (1) On both ends of the bearing, $P(0, \theta) = P(L, \theta) = P_a$
- (2) Pressure distribution is a symmetric function for centre of bearing length, $P(0 \rightarrow L/2, \theta) = P(L/2 \rightarrow L, \theta)$
- (3) Pressure distribution is a continuous at $\xi = 0$

(4) Pressure distribution is a periodic function,

$$P(\xi, \theta) = P(\xi, \theta + 2\pi), \quad \left. \frac{\partial P}{\partial \theta} \right|_{\theta} = \left. \frac{\partial P}{\partial \theta} \right|_{\theta + 2\pi}$$

B. Solution of Equations of Motion

Equation of motions of rotor supported by externally pressurized gas bearing is already given in (1) and (2). Dynamic motions of the rotor depend on to the flow of the air between the rotor and the bearing. So, an iterative procedure must be used to obtain radial motion of the rotor. Because at every iteration step fluid flow and so the supporting pressure on the rotor must be calculated. This procedure could be summarized as follows;

(1) When $t=0$, after the time increment Δt , the new value of acceleration, velocity and displacement of rotor is estimated forth order Runge-Kutta method and gap (H) between rotor and shaft is calculated with new value of displacement.

(2) New value of H the Reynold's equation are solved with mass flow through the orifice feeding. So a new pressure distribution is obtained in the gap between rotor and bearing.

(3) Pressure distribution is integrated over the rotor circumference and length; force distribution is estimated;

$$F_x = p_a R^2 \int_0^{2\pi} \int_0^{L/R} P(\xi, \theta) \cos \theta d\xi d\theta \tag{8}$$

$$F_y = p_a R^2 \int_0^{2\pi} \int_0^{L/R} P(\xi, \theta) \sin \theta d\xi d\theta$$

(4) The value of displacement and velocity from step 1, pressure distribution from step 2 and component force from step 3 to be new initial conditions for second time step. And then procedure returns to step 1 to calculate new state that will obtained in the time interval $\Delta t \rightarrow 2\Delta t$

IV. RESULTS AND DISCUSSION

In this section, effect of mass flow rate on the dynamics of externally pressurized gas lubricated bearing with different orifice diameter, number of orifice and radial clearances are analyzed. Bearing data used in the simulations are given in Table 1 and orifice locations are given in Fig. 2.

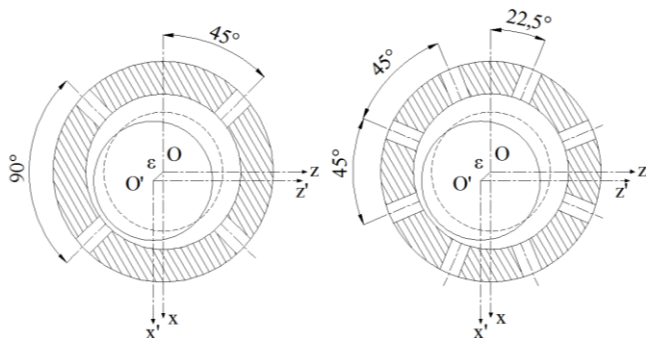


Fig. 2 Location of orifice on bearing a. 4 orifices b. 8 orifices

TABLE I
BEARING DETAIL

Symbol	Quantity	Value
L	Length, L	0.05 m
R	Radius, R	0.025 m
μ	Viscosity	17.4×10^{-6}
R^0	Gas constant	287.6 J/Kg.K
T^0	Absolute Temperature	288 °K

A. Pressure Distribution

Pressures values along the circumferential direction are given in Fig. 3 for 4 and 8 orifices on polar graphic. The pressure value decreases as radial clearance increased. This is reasonable because the gap volume increase for the same mass flow rate. So the pressure values of bearing which has small radial clearances are higher than the bearing with big radial clearances. In addition, the pressure values increase with the increase of supply ports, i.e. number of orifice.

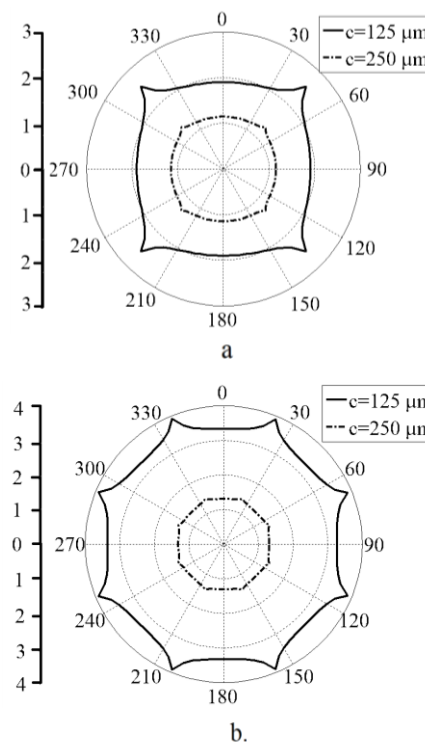


Fig. 3 Pressure distribution at 2 atm, $\epsilon = 0$ and $d_o = 0.003$ m a. 4 orifice b. 8 orifice

B. Mass Flow Rate

Mass flow rate is function of orifice diameter as well as clearance between rotor and bearing (Fig. 4). Mass flow rate increases with increasing orifice diameter and this also affect the bearing pressure distribution which is defined by Reynold's equation as seen in Fig. 4.

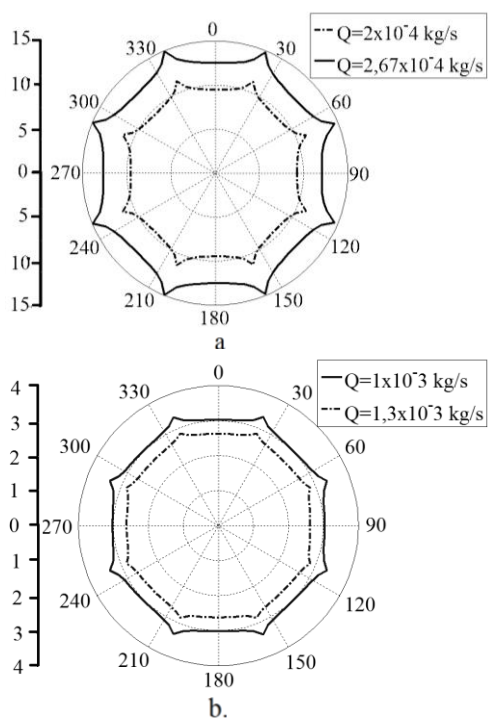


Fig. 4 Pressure distribution for different mass flow rate a. $c=50 \mu\text{m}$, b. $c=250 \mu\text{m}$ ($P_s=2 \text{ atm}$ and $\epsilon=0$)

Feeding parameter which is given in (4) is a function radial clearance and orifice diameter. So mass flow rate are affected by changing radial clearance and orifice diameter. Mass flow rates passing through an orifice for different orifice diameter and radial clearance are given in Fig. 5. It is clear that mass flow rate increases when radial clearance is increased. Besides, mass flow rate increases as orifice diameter is increased.

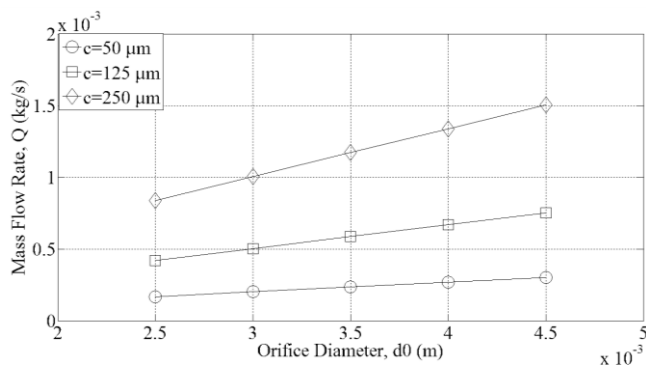


Fig. 5 Mass flow rate vs. orifice diameter for different radial clearance respectively $50 \mu\text{m}$, $125 \mu\text{m}$ and $250 \mu\text{m}$, ($P_s=2 \text{ atm}$)

Supply pressure also changes the mass flow rate. Fig. 6 shows the change of mass flow rate (Q) with supply pressure. The mass flow rate increase with increasing supply pressure, however, the slope of two line for different orifice diameters are different. Because the effect of orifice diameter on the feeding parameter is quadratic as seen at 4.

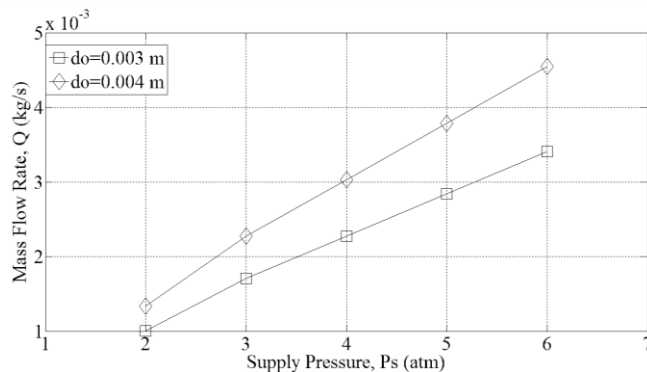


Fig. 6 Mass flow rate vs. supply pressure for different orifice diameter ($P_s=2 \text{ atm}$ and $c=125 \mu\text{m}$)

C. Load Carrying Capacity

Load carrying capacity is the sum of forces applied to the shaft produced by pressure distribution between shaft and bearing. It is affected by all of the parameters that effect the pressure distribution. And the load carrying capacity is directly related to the dynamic of rotor supported as defined in equation of motion which is given in (1).

In order to observe the effect of mass flow rate to the load carrying capacity a serial cases are simulated and results are given in Fig. 7 and Fig. 8. Load carrying capacity increases with increasing orifice diameter linearly (Fig. 7) due to increasing mass flow rate. As the number of orifice is increased, the mass flow rate increases (from 4 to 8) and on the load carrying capacity is significantly affected (almost doubled).

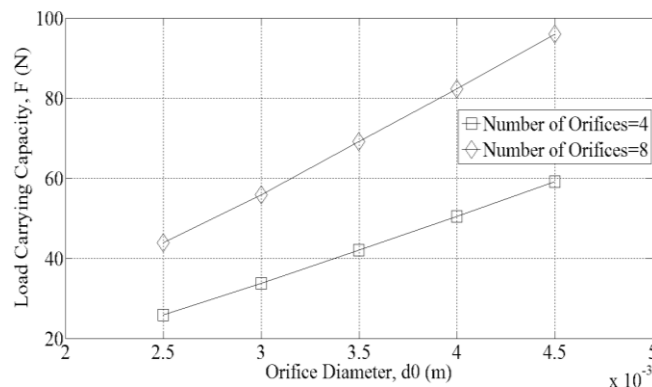


Fig. 7 Load carrying capacity vs. orifice diameter for different number of orifice ($P_s=2 \text{ atm}$ and $c=125 \mu\text{m}$)

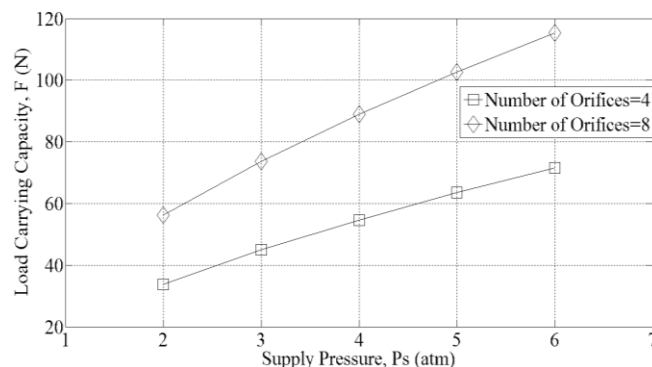


Fig. 8 Load carrying capacity vs. supply pressure for different number of orifices ($d_0=0.003 \text{ m}$ and $c=125 \mu\text{m}$)

D. Vibrations of Rotor

In simulations damping which is caused by supporting air is assumed to be constant in the range of the vibration amplitude. In the figures the transient part of the simulation are not given, but the steady state condition are shown. Fig. 9 and Fig. 10 shows vibration and orbital behaviour of the rotor for different orifice diameter respectively. Frequency of the vibration is increased with increasing orifice diameter. Because the orifice diameter is increased the load carrying capacity which is directly related to the stiffness of the air bearings. On the other hand vibration amplitude is increased with orifice diameter. Because rotor is excited around its resonance region due to selected parameters

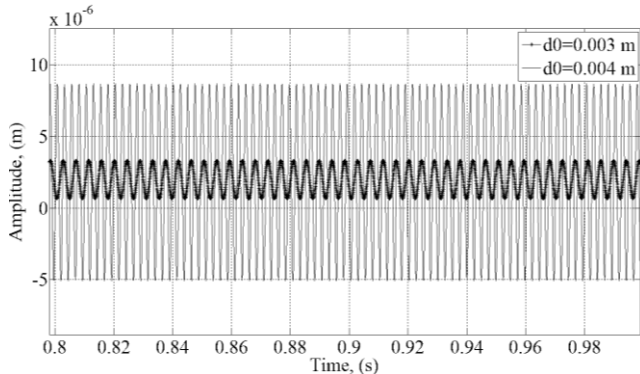


Fig. 9 Vibration of rotor at x-direction, $P_s=2$ atm and $c=125 \mu\text{m}$ (Number of orifice is 4)

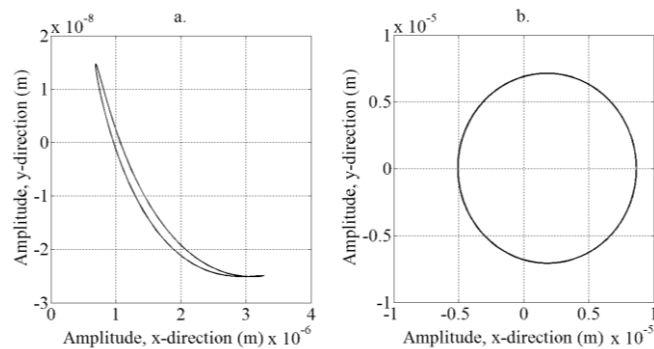


Fig. 10 Orbit of the rotor centre, $P_s=2$ atm and $c=125 \mu\text{m}$, a. $d_o=0,003$ m, b. $d_o=0,004$ m

Fig. 11 and Fig. 12 shows vibration and orbital behaviour of the rotor for different supply pressure respectively. Frequency of the vibration is increased with increasing supply pressure. However vibration amplitude is decreased with increasing supply pressure, because rotor is excited out off its resonance region with the selected parameters.

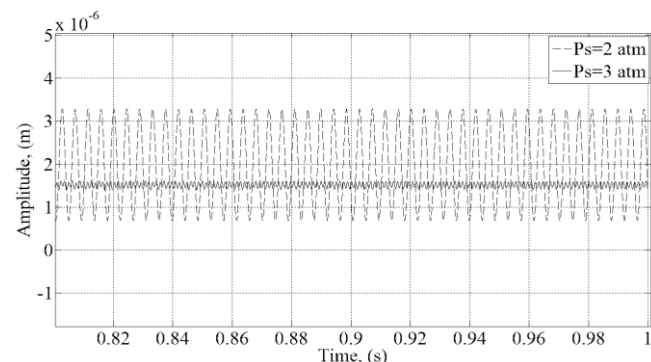


Fig. 11 Vibration of rotor at x-direction, $d_o=0,003$ m and $c=125 \mu\text{m}$ (Number of orifice is 4)

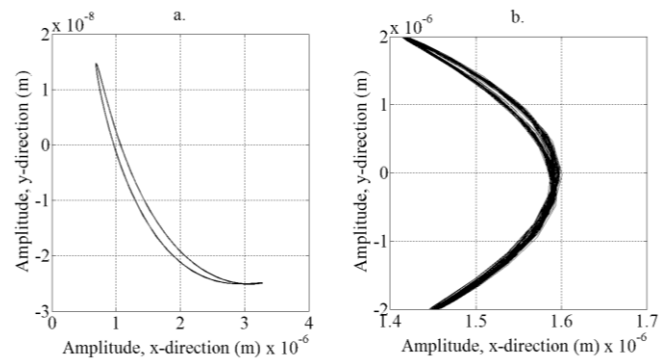


Fig. 12 Orbit of the rotor center, $d_o=0.003$ m and $c=125 \mu\text{m}$, a. $P_s=2$ atm, b. $P_s=3$ atm

V. CONCLUSION

In this paper, effect of mass flow rate on dynamics of rotor and characteristics of an externally pressurized gas bearing are investigated for high values of clearance. In order to obtain dynamic simulation of the rotor, first of all Reynold's equation is solved with alternating direction implicit scheme and the bearing and then two degree of freedom mathematical model of the rotor system is simulated for different supply pressures, clearances, orifice diameters and number of orifices. Results show that;

- increasing number of orifices is increases the load carrying capacity
- the load carrying capacity could also be increased by increasing the supply pressure
- the load carrying capacity could be increased by increasing the diameter of the orifice diameter.
- the load carrying capacity is a direct measure of bearing stiffness, so selection of the bearing dimensions and working parameters directly effects the dynamics of the rotor supported

Air bearing with a clearance of $125 \mu\text{m}$ could easily be achieved using conventional manufacturing methods. And results suggest that externally pressurized gas bearings which have higher value of radial clearances could still be used to support a rotor, although it has low load carrying capacity.

APPENDIX A

Before Reynold's equation is discretized, it can rearrange with taking derivative into following form;

$$-3H^2 \left(\frac{\partial H}{\partial \theta} \frac{\partial \Theta}{\partial \theta} + \frac{\partial H}{\partial \xi} \frac{\partial \Theta}{\partial \xi} \right) - H^3 \left(\frac{\partial^2 \Theta}{\partial \theta^2} + \frac{\partial^2 \Theta}{\partial \xi^2} \right) + \frac{\Lambda H}{P} \frac{\partial \Theta}{\partial \theta} + 2\Lambda P \frac{\partial H}{\partial \theta} + \frac{\sigma H}{P} \frac{\partial \Theta}{\partial t} + 2\sigma P \frac{\partial H}{\partial t} = 2\dot{M}$$

The right side of this equation terms is different zero for the orifice inlet point and the corresponding boundary conditions using the alternating direction implicit scheme in the $M \times N$ uniform grid with the circumferential and axial coordinates (Fig. A).

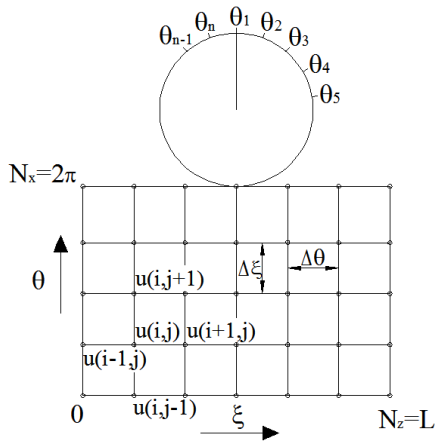


Fig. A Grid Scheme for air film

In this scheme at ξ direction the following formula are applied;

$$\begin{aligned} & \sigma \frac{H_{ij}^n}{P_{ij}^n} \frac{\Theta_{ij}^{\frac{n+1}{2}} - \Theta_{ij}^n}{\Delta t} + 2\sigma P_{ij}^n \frac{H_{ij}^{\frac{n+1}{2}} - H_{ij}^n}{\Delta t} \\ & + 2\Lambda \frac{\Theta_{ij}^n}{P_{ij}^n} \frac{H_{i,j+1}^{\frac{n+1}{2}} - H_{i,j-1}^n}{2\Delta\theta} + \Lambda \frac{H_{ij}^n}{P_{ij}^n} \frac{\Theta_{i,j+1}^n - \Theta_{i,j-1}^n}{2\Delta\theta} \\ & - 3(H_{ij}^n)^2 \frac{(H_{i,j+1}^n - H_{i,j-1}^n)(\Theta_{i,j+1}^n - \Theta_{i,j-1}^n)}{4\Delta\theta^2} - (H_{ij}^n)^3 \frac{(\Theta_{i,j+1}^n - 2\Theta_{ij}^n + \Theta_{i,j-1}^n)}{\Delta\theta^2} \\ & - 3(H_{ij}^n)^2 \frac{(H_{i+1,j}^n - H_{i-1,j}^n)(\Theta_{i+1,j}^{\frac{n+1}{2}} - \Theta_{i-1,j}^{n+1})}{4\Delta\xi^2} \\ & - (H_{ij}^n)^3 \frac{(\Theta_{i+1,j}^{\frac{n+1}{2}} - 2\Theta_{ij}^{\frac{n+1}{2}} + \Theta_{i-1,j}^{\frac{n+1}{2}})}{\Delta\xi^2} = \dot{M} \end{aligned}$$

where $\Theta = P^2$ and ADI scheme for the second stage at θ direction can be applied similarly. Then all the equations may be into a tri-diagonal matrix and solved using iterative method.

ACKNOWLEDGMENT

This study was supported by The Scientific and Technology Research Council of Turkey under Grant No 112M847.

REFERENCE

- [1] Fleming, D., Cunningham P. and Anderson, W. J., 1968 "Stability Analysis For Unloaded Externally Pressurized Gas-Lubricated Bearings With Journal Rotation," Technical Report, TN D-4934, NASA Lewis Research Center, United States.
- [2] Fourka, M. and Bonis, M., 1997, "Comparison between externally pressurized gas thrust bearings with different orifice and porous feeding systems", *Wear*, Vol. 210 (1997), pp. 311-317.
- [3] Renn, J-C., Hsiao, C-H., 2004, "Experimental and CFD study on the mass flow-rate characteristic of gas through orifice-type restrictor in aerostatic bearings", *Tribology International*, Vol. 37 (2004), pp. 309-315.
- [4] Lo, C., Wang, C. and Lee, Y., 2005, "Performance Analysis Of High-Speed Spindle Aerostatic Bearings," *Tribology International*, Vol. 38, pp. 5-14.
- [5] Colombo, F., Raparelli, T. and Viktorov, V., 2009a, "Externally Pressurized Gas Bearings: A Comparison Between Two Supply

- Holes Configurations," *Tribology International*, Vol. 42, pp. 303-310.
- [6] Colombo, F., Raparelli, T. and Viktorov, V., 2009b, "Comparison Between Different Supply Port Configurations In Gas Journal Bearings," *New Tribological Ways*, Vol. 23, pp. 477-498.
- [7] Chen, Y., S., Chiu, C., C. and Cheng, Y., D., 2010, "Influences of operational conditions and geometric parameters on the stiffness of aerostatic journal bearings," *Precision Engineering*, Vol. 34, pp. 722-734.
- [8] Belforte, G., Raparelli, T., Trivella, A. and Viktorov, V., 2010, "Identification Of Discharge Coefficients Of orifice-Type Restrictors For Aerostatic Bearings and Application Examples," *New Tribological Ways*, Vol. 18, pp. 359-380.
- [9] Czolczynski, K., 1999, "Mathematical Model of a Gas Journal Bearing," *Rotordynamics of Gas-Lubricated Journal Bearing System*, Vol 1, pp.11-22.
- [10] Douglas, J., J., and Kim, S, 1999, "On accuracy of alternating direction implicit methods for parabolic equations," *Preprint*
- [11] Al-Rozbayani, A., and Yahya, M., 2012, "Alternating Direction Implicit Method for Solving Parabolic Partial Differential Equations in Three Dimensions," *Raf. J. of Comp. & Math's*, Vol. 9, pp.79-97.
- [12] Chapra, S., C., and Canale, P., R., 1998, "Partial Differential Equation," *Numerical Methods for Engineers*, Vol.3, pp.832-848.
- [13] Belforte, G. C., Raparelli, T., Viktorov, V., 1999, "Theoretical Investigation of Fluid Inertia Effects and Stability of Self-Acting Gas Journal Bearings," *Journal of Tribology*, Vol. 121, pp. 836-843.